Desalination and Water Treatment
www.deswater.com

doi: 10.5004/dwt.2018.22506

121 (2018) 284–290
July

Studies on fluidization of sand particles in a three-phase stirred fluidized bed using response surface methodology

N. Deepa Priya*, K. Saravanan, R. Akshaya

Department of Chemical Engineering, Kongu Engineering College, Perundurai – 638060, India, Tel. +918056542401; email: dppriya1984@gmail.com (N. Deepa Priya), Tel. +919786605656; email: rumisivaesh@yahoo.com (K. Saravanan), Tel. +919080120393; email: akshayarajasekaran21@gmail.com (R. Akshaya)

Received 28 February 2018; Accepted 15 May 2018

ABSTRACT

Fluidized beds have been extensively used in chemical and process industries because of several advantages like high rate of heat and mass transfer, low pressure drops and uniform temperature distribution. Enhanced heat and mass transfer and gas–solid contact can be attained only by good fluidization quality. However maintaining the fluidization quality is difficult due to the factors such as particle size distribution and fluid–solid density ratio. In order to overcome these difficulties, mechanical stirring is attempted. The present study is directed to analyse the effects of gas velocity, bed height and stirring speed, on pressure drop and power in a stirred fluidized bed with air–water–sand system using response surface methodology. The Box–Behnken method was applied to optimize the effects of the operating parameters, including gas velocity (0.03–0.07 m/s), bed height (0.08–0.12 m) and stirring speed (600–1,400 rpm) on responses pressure drop (N/m^2) and power (W). It was observed that initially pressure drop increases with gas velocity but subsequently it starts decreasing because the bubble rise will be high due to upward force. As the gas velocity and bed height was increased, there will be decrease in porosity, which results in decrease in pressure drop and power. As the stirring speed increases, the pressure drop and power increases, as power is proportional to third power of impeller speed. Optimized conditions of bed height, air flow rate and stirrer speed were found to be 0.03 m/s, 0.08 m and 600 rpm, respectively. The minimum fluidization velocity was calculated and the calculated result was found to be in good agreement with the visually observed value.

Keywords: Stirred fluidized bed; Sand particles; Response surface methodology; Pressure drop

1. Introduction

Fluidization process occurs when a fluid is passed up through the granular material. Presently fluidized bed is widely used in variety of applications including fluid catalytic cracking, polymer synthesis, gasification of coal and biomass, adsorption, chemical conversions, drying and several other processes [1–3]. Efficient contact between the solid and fluid phases, thermal homogeneity and better heat and mass transfer are some of the advantages of fluidized beds [4,5]. Excellent fluidization quality is essential for ensuring gas–solid contact and mass transfer. However, it is tough to maintain smooth fluidization because of particle size distribution which causes channelling and agglomeration of particles, that is, usually fine particles tend to agglomerate [6]. Another factor disturbing fluidization is fluid–solid density ratio, especially gas-solid beds shows large heterogeneities leading to bubble formation, agglomeration and channelling. The fluidization quality can be improved by aeration of the bed, but excessive aeration leads to bubble formation and slugging. In this juncture, aeration accompanied with mechanical stirring was introduced to fluidized beds to improve the performance

* Corresponding author.

Presented at the 3rd International Conference on Recent Advancements in Chemical, Environmental and Energy Engineering, 15–16 February, Chennai, India, 2018

of fluidization. Stirring the bed induces the energy required to break down interparticle bonds, minimizes agglomerates and helps in eliminating channelling.

Very few works have been reported in the literature on stirred fluidized bed. Leva [7] studied the effect of positioning of blades, stirrer height and stirrer speed in a stirred fluidized bed. He observed that a sharp effect on pressure drop is noted when the blades are at an angle of 135° and 90°, 4 blade stirrer was essentially active in the base of the column, with the 8 blade stirrer, the effects became much more pronounced, especially at high speed and with 11 blades, the effects became even greater. He also reported that the pressure drop increases with the increase in stirrer speed and power increases with the aeration rate.

Stirred fluidized bed finds wide application in chemical, biotechnology, pharmaceutical, food and other industries. Stirred fluidized bed is an attractive device for segregation [8] of solid particles but the segregation rate may be low. Stirring decreases the minimum fluidization velocity, porosity and increases the bulk density of the bed [9]. When solid–solid reactions are carried out in a stirred fluidized bed the reaction time to get the required conversion is decreased, there is increase in the rate of heat transfer and rate of reaction [10]. Lysozyme can be directly recovered from chicken egg white by using stirred fluidized bed. When compared with the expanded bed absorption technology, the stirred fluidized bed technique gives high yield of lysozyme with a high purification factor [11]. Stirred fluidized bed along with vibration can completely eliminate channelling and agglomeration and this is an attracting device for gas–solid reactions of Geldart C powders such as potato starch [12,13].

The present work is focussed to study the hydrodynamics of stirred fluidized bed using sand–air–water system. In three-phase fluidized beds, there is sufficient contact between the phases, hence it has several advantages such as excellent axial dispersion, temperature uniformity, heat transfer enhancement, mixed flow patterns, etc. [14]. Three-phase fluidized beds find application in wastewater treatment [15], electrochemical process, etc. Minimum fluidization velocity (U_{mf}) was predicted to examine the effect of stirring on the fluidization characteristics of the particles. This work also involves the investigation of the effect of air flow rate, bed height and stirrer speed on pressure drop and power.

2. Materials and methods

Experimental setup is shown in Fig. 1 which is made up of transparent acrylic with an inner diameter of 50 mm, outer diameter of 60 mm and height of 1,000 mm. In order to increase the efficiency of mixing, a stirrer is employed. For this purpose, four impeller designs are fabricated and tested against hydrodynamic parameters. These impellers are made up of stainless steel with a diameter of 7 mm. Impellers used in the present study are roustion turbine – 1 number, pitched blade [16] down flow 45° – 4 numbers, pitched blade up flow – 1 number. A pre-calibrated rotameter is fitted to measure the flow rate of liquid and air in the range of 0–5 LPM for liquid and 0–10 LPM for air. A U-tube differential manometer is used to measure the pressure drop, which is fixed across the column. The whole setup is mounted on movable trolley. Compressed air is passed to the system through compressor (5 HP). For each parameter four to six readings are taken to maintain the consistency and accuracy.

Water is introduced into the bed at 2 LPM and it flows continuously. Air was introduced at the bottom of the bed and the pressure drop was measured using a differential manometer. Impeller speed is measured using digital tachometer. The physical properties of the particles used in the experiment are shown in Table 1. The particle size distribution of sand is shown in Table 2. Since the mass of particle retained in mesh numbers 52, 60 and 85 is more, we have chosen the particles retained in the sieve for our study and the average particle diameter in the sieves was 0.36, 0.275 and 0.215 mm which was rounded as 0.4, 0.3 and 0.2 mm.

3. Results and discussion

3.1. Prediction of minimum fluidization velocity

The main parameter to identify the characteristics of fluidized bed is the minimum fluidization velocity. Kozeny–Carman equation was used by Marring et al. [17] and Ergun equation was used by Mawatari et al. [18] to predict the minimum fluidization velocity in a vibrated fluidized bed. In this study, the minimum fluidization velocity (u_{mf}) was calculated by the following correlation developed from Ergun equation,

$$u_{mf} = 0.0055 \frac{\in_m^3}{(1-\in_m)} \frac{D_p^2(\rho_p - \rho_g)}{\mu_g} g \quad (1)$$

where $\in_m$ is the porosity at minimum fluidization, Φ_s is the sphericity of the particle, D_p is the particle diameter in m, ρ_p is the particle density in kg/m³, ρ_g is the gas density in kg/m³, μ_g is the gas viscosity in kg/ms. By visual observation,

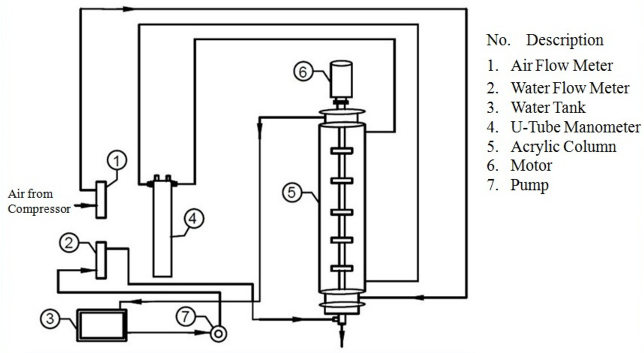

Fig. 1. Stirred fluidized bed.

Table 1
Properties of solid (sand) and liquid (water)

Property	Value
Density of water, ρ_p in kg/m³	1,000
Density of sand, ρ_p in kg/m³	1,600
Diameter of sand, D_p in mm	0.3
Sphericity of sand	**1**
Porosity of sand	**0.395**
Loading (%)	8, 10, 12

Table 2
Particle size distribution of sand

S. No.	Mesh No.	Screen opening size, D_{pi} (mm)	Mass retained (g)	Average diameter of particle retained $\overline{D_{pi}}$ (mm)
1.	18	0.850	110	–
2.	35	0.420	208	0.635
3.	52	0.300	625	0.360
4.	60	0.250	492	0.275
5.	85	0.180	340	0.215
6.	100	0.150	118	0.165
7.	150	0.106	78	0.128
8.	200	0.074	20	0.090
9.	Pan	–	08	–

the minimum fluidization velocity is found to be 0.08 m/s and the calculated value is 0.0487 m/s with a deviation of ±4%. The minimum fluidization velocity of stirred fluidized bed is considerably reduced when compared with conventional fluidized bed. The same result was reported by Zhou et al. [19].

The effect of superficial velocity on pressure drop across the bed is presented in Fig. 2. It is observed that the pressure drop decreases with increase in superficial gas velocity for both stirred and unstirred conditions of the bed, the same effect was observed by Lee et al. [20], Buffière and Moletta [21] and Legile [22]. This is because of the increase in fractional gas holdup, and hence a decrease in the bulk density of the bed, with increase in superficial gas velocity. It is also noticed that for a given superficial gas velocity, the pressure drop across the bed is lower for the stirred bed than that for the unstirred bed. This effect is due to the fact that the size of the bubble is reduced due to stirring which, in turn, increases the fractional gas holdup and decreases the bulk density of the bed.

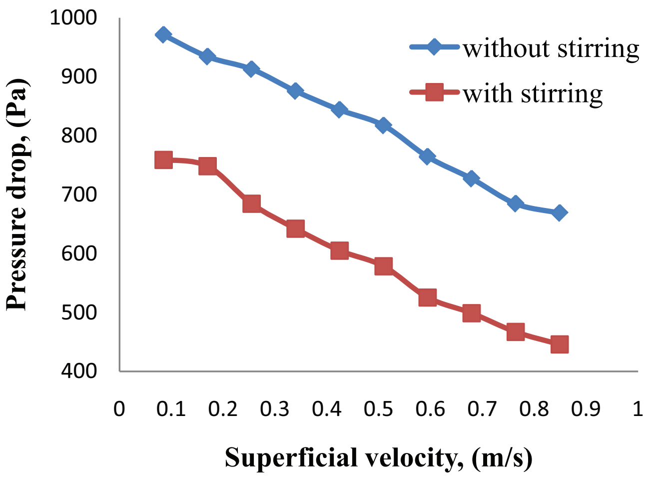

Fig. 2. Plot of pressure drop vs. superficial velocity with stirring and without stirring.

3.2. Box–Behnken design and analysis

Response surface methodology is an efficient tool for statistical analysis which has been used to optimize multiple variables with lesser number of experiments thereby optimal conditions for complex solutions can be arrived [23,24]. Response surface methodology was used to find the effect of gas velocity, bed height and stirring speed on pressure drop (ΔP) and power (P). To optimize the variables and to generate the response surface plots based on commercial statistical package [25] (Design of Experiments software: Design-Expert 8.0.7.1), response surface methodology [26] was applied to the experimental data [27]. The experiments on fluidization characteristics of sand particles were designed in Box–Behnken Design using three factors with three levels. The levels or range of factors were selected appropriately based on parametric studies of previously conducted experiments. The different levels of factors considered for experimentation is given in Table 3. The number of experiments (N) required for the development [28] of Box–Behnken design is defined as $N = 2k(k-1) + C_o$, where k is the number of factors and C_o is the number of central points. With different combinations, a total of 17 runs were conducted for the study. Analysis of variance [29] provides comparison between variations caused by experimental runs and variations caused by measurement errors thereby contribution of each terms in regression and significance of the model equations can be identified. By keeping the third factor constant, response surface plots were arrived as a function of two parameters. Response surface plots will give accurate geometrical representation thereby enabling to assess the behavioural system of the experimental design. The results of different trials with responses are presented in Table 4.

Table 3
Different levels of variables used for study

Factors	Name of the variable	Variable symbol	Minimum level (–1)	Maximum level (+1)
A	Gas velocity	V, m s^{-1}	0.03	0.07
B	Bed height	BH, m	0.08	0.12
C	Stirring speed	S, rpm	600	1,400

3.3. Effect of gas velocity, bed height and stirring speed on pressure drop

The result of the analysis of variance test as generated from the experimental data is shown in Table 4. Fitting of the data to various models was done to acquire regression equations. The accuracy of the model is tested by sequential model sum of squares and model summary statistics tests

Table 4
Experimental runs (generated by Box–Behnken design) and observed results of response variables

Run	Coded variables			Uncoded variables			Responses	
	V (*A*)	BH (*B*)	*S* (*C*)	*V* (*A*)	BH (*B*)	*S* (*C*)	ΔP (N m^{-2})	*P* (J s^{-1})
1	1	0	0	0.05	0.10	1,000	154.68	0.016
2	1	1	–1	0.05	0.12	600	171.87	0.018
3	1	1	1	0.05	0.12	1,400	194.79	0.02
4	1	0	0	0.05	0.10	1,000	154.68	0.016
5	–1	–1	0	0.03	0.08	1,000	114.58	0.008
6	–1	1	0	0.03	0.12	1,000	183.33	0.013
7	1	0	0	0.05	0.10	1,000	154.68	0.016
8	–1	0	1	0.03	0.10	1,400	166.14	0.011
9	1	0	0	0.05	0.10	1,000	154.68	0.016
10	0	–1	0	0.07	0.08	1,000	126.04	0.017
11	1	0	0	0.05	0.10	1,000	154.68	0.016
12	1	–1	–1	0.05	0.08	600	126.04	0.013
13	–1	0	–1	0.03	0.10	600	131.77	0.009
14	1	–1	1	0.05	0.08	1,400	143.23	0.015
15	0	0	–1	0.07	0.10	600	91.67	0.013
16	0	0	1	0.07	0.10	1,400	120.31	0.016
17	0	1	0	0.07	0.12	1,000	137.5	0.019

and the results are presented in Table 5. The significance of each variable was analyzed using Fisher's statistical test. From table, it was found that Prob > *F* value is found to be less than 0.0001, which means that the model is most significant. The bed height has the highest *F*-value and the lowest Prob > *F* value. This shows that bed height has the largest effect on pressure drop, followed by gas velocity and stirring speed. The model *F*-value was found to be 18.73 from the statistical analysis and the model was significant. The coefficient of determination (R^2) of 0.9601 was also found to be significant. Fitting of data was done by using different models and the quadratic model was found to be most significant. The model equation in coded form for the pressure drop is expressed as follows:

$$\begin{aligned}\text{Pressure Drop} &= +154.68 - 15.04 \times A + 22.20 \times B \\ &+ 12.89 \times C - 14.32 \times A \times B - 1.43 \times A \times C \\ &+ 1.43 \times B \times C - 22.91 \times A^2 + 8.60 \times B^2 \\ &- 4.29 \times C^2\end{aligned} \tag{2}$$

where *A* is gas velocity in m/s, *B* is bed height in m and *C* is stirring speed in rpm.

Table 5
ANOVA for pressure drop

Source	Sum of squares	d*f*	Mean square	*F* value	*p*-value Prob > *F*
Model	10,468.89	9	1,163.21	18.73	0.0004
A – gas velocity	1,809.01	1	1,809.01	29.13	0.0010
B – bed height	3,942.72	1	3,942.72	63.48	<0.0001
C – stirring speed	1,329.22	1	1,329.22	21.40	0.0024
AB	820.54	1	820.54	13.21	0.0083
AC	8.21	1	8.21	0.13	0.7269
BC	8.21	1	8.21	0.13	0.7269
A^2	2,210.69	1	2,210.69	35.59	0.0006
B^2	311.14	1	311.14	5.01	0.0602
C^2	77.63	1	77.63	1.25	0.3005
Cor total	10,903.64	16			
R^2 = 0.9601					

Fig. 3 indicates the effects of bed height, gas velocity and stirrer speed on pressure drop. It was observed that the pressure drop increases with the increase in bed height and bed stirring speed. With the increase in bed height of the column, pressure drop increases due to decrease in porosity. Bed porosity is faster for bed of static condition. The porosity increases with increase in gas velocity, hence the porosity starts increases when the bed attains the minimum fluidization condition. The expected porosity value at minimum fluidization condition will be 0.6 and it decreases with the increase in fluid velocity. On the other hand, the porosity value reaches maximum when the bed is at maximum fluidization condition and expected value will be 0.9. With increase in velocity, the pressure drop was constant till a particular velocity, 0.04 m/s, and then it starts decreasing. When the velocity is low the bubble size is low, hence the bubble rise is low. When the velocity increases, the gas bubbles become large, the combination of buoyant force and drag force is high, the resultant force predominates in upward direction and the bubble rise is high, this leads to decrease in pressure drop. Pressure drop increases with increase in stirring speed, as from power number, power is proportional to the third power of impeller speed. The same effects have been reported by Joshi and Sharma [30] in the studies on gas inducing type contacting agitators and by Kim and Han [31] in the studies on fluidization characteristics of fine particles.

3.4. Effect of gas velocity, bed height and stirring speed on power

The results of the analysis of variance shown in Table 6 indicated that the regression is significant due to the *F*-value of 22.55 and the Prob > *F* is found to be less than 0.0001 and the model is found to be most significant. The gas velocity has the highest *F*-value and the lowest Prob > *F* value. The gas velocity has the largest effect on power, followed by bed height and stirring speed. The model *F*-value was found to be 22.55 from the statistical analysis and the model was significant. The coefficient of determination (R^2) of 0.9667 was also found to be significant. The model equation for the power is expressed as follows:

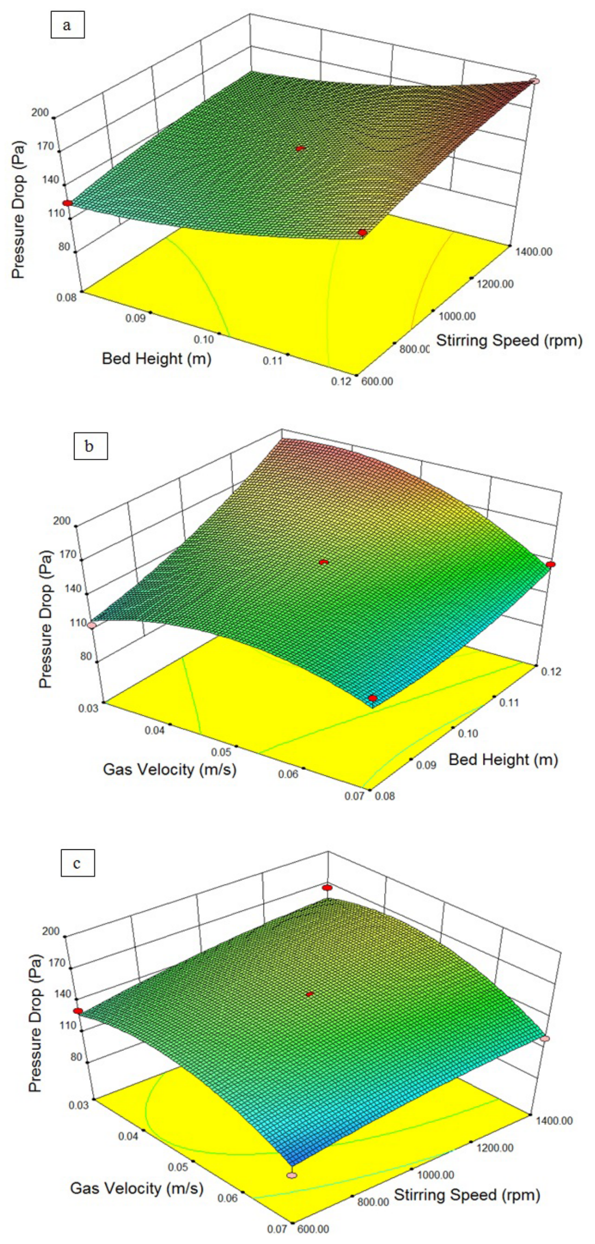

Fig. 3. (a) Effect of bed height and stirring speed on pressure drop; (b) effect of gas velocity and bed height on pressure drop; (c) effect of gas velocity and stirring speed on pressure drop.

$$\begin{aligned}\text{Power} = {} & +0.016 + 3.000\text{E}-003\times \text{A} + 2.125\text{E}-003\times \text{B} \\ & +1.125\text{E}-003\times \text{C} - 7.500\text{E}-004\times \text{A}\times \text{B} \\ & +2.500\text{E}-004\times \text{A}\times \text{C} \\ & + 0.000\times \text{B}\times \text{C} - 3.000\text{E}-003\times \text{A}^2 \\ & + 1.250\text{E}-003\times \text{B}^2 - 7.500\text{E}-004\times \text{C}^2\end{aligned} \quad (3)$$

where *A* is gas velocity in m/s, *B* is bed height in m and *C* is stirring speed in rpm.

Fig. 4 indicates the effects of bed height, gas velocity and stirrer speed on power. It was observed that the power increases with the increase in bed height and stirring speed, this is due to decrease in porosity. Power is proportional to the third power of impeller speed (Joshi and Sharma [30]), hence there is increase in power with stirring speed. Power increases with increase in velocity up to the velocity 0.06 m/s, and then it starts decreasing. Figs. 5(a) and (b) show parity plot which compares the experimental values with predicted values of pressure drop and power. The model is found to be significant as there is good correlation between experimental and predicted values.

4. Conclusions

Fluidization studies were carried out in three-phase fluidized bed using sand–water–air system. The performance of the fluidized bed can be improved with the use of stirrer. The visually observed and calculated values of minimum fluidization velocity are compared and the deviation was found to be only ±4%. The pressure drop across the bed is lower for stirred bed than unstirred bed, because the bubble size gets reduced on stirring, which results in increase in fractional holdup and decrease in bulk density of bed. Pressure drop and power increases with gas velocity and bed height, due to decrease in porosity. As the gas velocity increases, the pressure drop increases till a particular velocity, then it starts decreasing. This is because, the bubbles becomes large when the velocity is increased, at this time the combination of buoyant and drag force is high and it predominates in the upward direction and the bubble rise will be high, hence

Table 6
ANOVA for power

Source	Sum of squares	df	Mean square	F value	p-value Prob > F
Model	1.667E-004	9	1.852E-005	22.55	0.0002
A-gas velocity	7.200E-005	1	7.200E-005	87.65	<0.0001
B-bed height	3.612E-005	1	3.612E-005	43.98	0.0003
C-stirring speed	1.012E-005	1	1.012E-005	12.33	0.0098
AB	2.250E-006	1	2.250E-006	2.74	0.1419
AC	2.500E-007	1	2.500E-007	0.30	0.5983
BC	0.000	1	0.000	0.000	1.0000
A^2	3.789E-005	1	3.789E-005	46.13	0.0003
B^2	6.579E-006	1	6.579E-006	8.01	0.0254
C^2	2.368E-006	1	2.368E-006	2.88	0.1333
Total	1.725E-004	16			
R^2 = 0.9667					

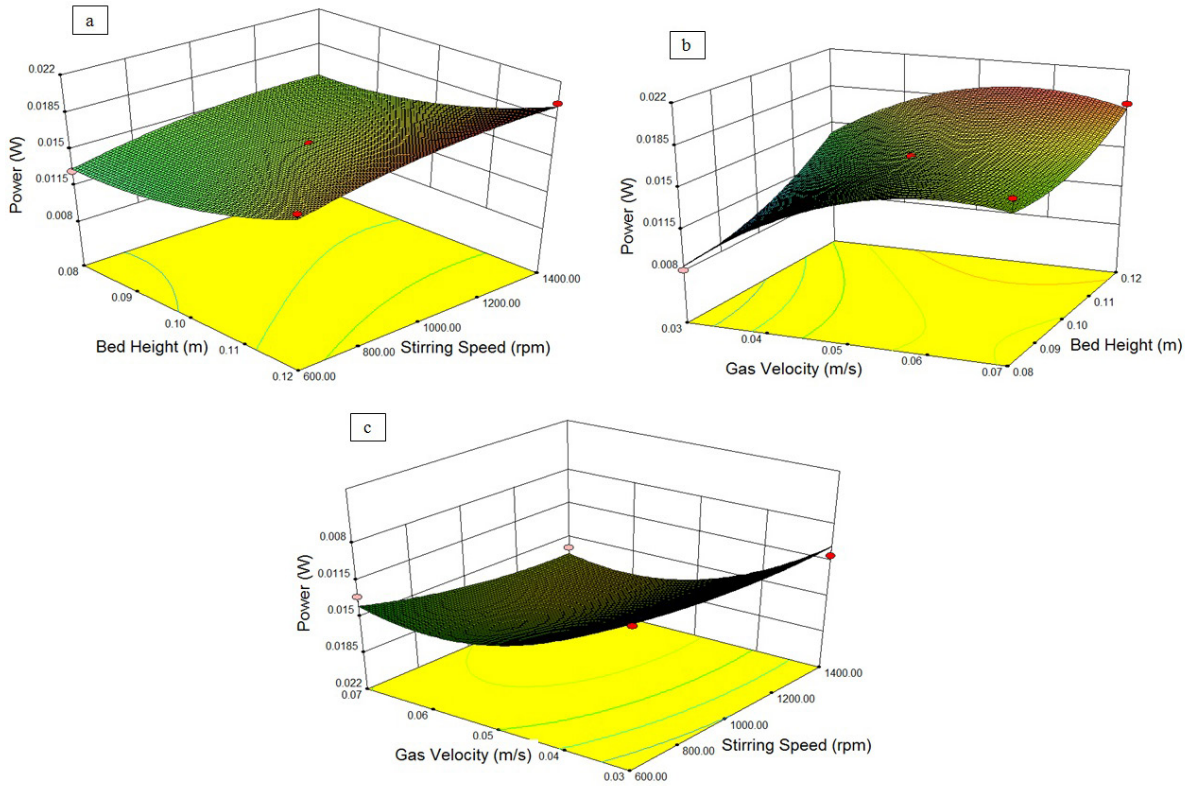

Fig. 4. (a) Effect of bed height and stirring speed on power; (b) effect of gas velocity and bed height on power; (c) effect of gas velocity and stirring speed on power.

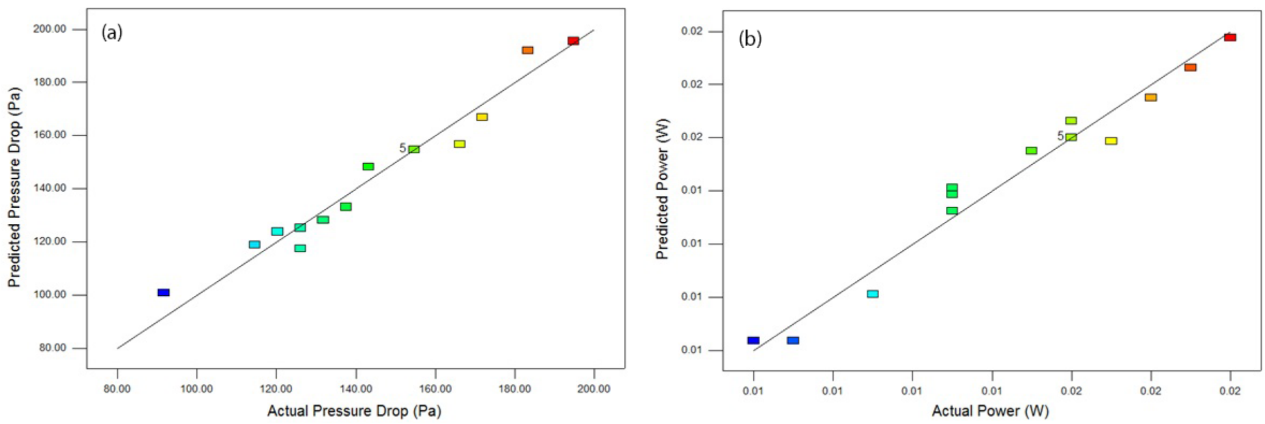

Fig. 5. (a) Parity plot for pressure drop and pressure drop. (b) Parity plot for pressure drop and power.

there is decrease in pressure drop. Pressure drop and power consumption increases with the increase in stirring speed, as power is proportional to third power of impeller speed. The parameters such as bed height, gas velocity and stirring speed were optimized using Box–Behnken design of experiments to obtain low pressure drop and less power. The optimized values of gas velocity, bed height and stirring speed were found to be 0.03 m/s, 0.08 m and 600 rpm, respectively.

References

[1] D. Kunii, O. Levenspiel, Fluidization Engineering, Elsevier, New York, 2013.

[2] N.D. Priya, S.M. Pradeep, K. Saravanan, Hydrodynamics and CFD modeling of food materials using circulating fluidized bed, Int. J. ChemTech Res., 10 (2017) 276–288.

[3] A. Anjana Anand, S. Adish Kumar, J. Rajesh Banu, G. Ginni, The performance of fluidized bed solar photo Fenton oxidation in the removal of COD from hospital wastewaters, Desal. Wat. Treat., 57 (2016) 8236–8242.

[4] J. Medrano, M. Tasdemir, F. Gallucci, M. van Sint Annaland, On the internal solids circulation rates in freely-bubbling gas-solid fluidized beds, Chem. Eng. Sci., 172 (2017) 395–406.

[5] N.D. Priya, K. Saravanan, S.M. Pradeep, N. Subramnaian, Studies on hydrodynamics of food grains in a circulating fluidized bed, Int. J. Adv. Res. Technol., 2 (2013) 73–77.

[6] J.R. van Ommen, J.M. Valverde, R. Pfeffer, Fluidization of nanopowders: a review, J. Nanopart. Res., 14 (2012) 737.

[7] M. Leva, Pressure drop and power requirements in a stirred fluidized bed, AIChE J., 6 (1960) 688–692.
[8] D. Su, Z. Luo, L. Lei, Y. Zhao, Segregation modes, characteristics, and mechanisms of multi-component lignite in a vibrated gas-fluidized bed, Int. J. Mining Sci. Technol., 28 (2017) 251–258.
[9] Z. Zhang, J. Beeckmans, Segregation in a stirred fluidized bed, Can. J. Chem. Eng., 68 (1990) 932–937.
[10] J. Murthy, V. Surendar Reddy, T. Sankarshana, Solid–solid reaction in a fluidized bed, Asia-Pacific J. Chem. Eng., 6 (2011) 244–256.
[11] Y.-K. Chang, I.-P. Chang, Method development for direct recovery of lysozyme from highly crude chicken egg white by stirred fluidized bed technique, Biochem. Eng. J., 30 (2006) 63–75.
[12] N. Kuipers, E. Stamhuis, A. Beenackers, Fluidization of potato starch in a stirred vibrating fluidized bed, Chem. Eng. Sci., 51 (1996) 2727–2732.
[13] D. Geldart, Types of gas fluidization, Powder Technol., 7 (1973) 285–292.
[14] P.R. Kumar, B.N. Rao, P. Venkateswarlu, K. Ramesh, Wall-to-bed mass transfer in a three-phase fluidized bed with coaxially placed string of spheres internal, Mater. Today Proc., 5 (2018) 470–476.
[15] X. Wang, M. Liu, Z. Yang, Coupled model based on radiation transfer and reaction kinetics of gas-liquid-solid photocatalytic mini-fluidized bed, Chem. Eng. Res. Design, 134 (2018) 172–185.
[16] D. Devakumar, K. Saravanan, Study and design of impellers for multiphase reactors, Modern Appl. Sci., 2 (2008) 99.
[17] E. Marring, A. Hoffmann, L. Janssen, The effect of vibration on the fluidization behaviour of some cohesive powders, Powder Technol., 79 (1994) 1–10.
[18] Y. Mawatari, Y. Tatemoto, K. Noda, Prediction of minimum fluidization velocity for vibrated fluidized bed, Powder Technol., 131 (2003) 66–70.
[19] E. Zhou, Y. Zhang, Y. Zhao, Z. Luo, J. He, C. Duan, Characteristic gas velocity and fluidization quality evaluation of vibrated dense medium fluidized bed for fine coal separation, Adv. Powder Technol., 29 (2018) 985–995.
[20] D.-H. Lee, N. Epstein, J.R. Grace, Hydrodynamic transition from fixed to fully fluidized beds for three-phase inverse fluidization, Korean J. Chem. Eng., 17 (2000) 684–690.
[21] P. Buffière, R. Moletta, Some hydrodynamic characteristics of inverse three phase fluidized-bed reactors, Chem. Eng. Sci., 54 (1999) 1233–1242.
[22] P. Legile, Contribution to the study of an inverse three-phase fluidized bed operating counter-currently, Int. Chem. Eng. J., 32 (1992) 41–50.
[23] M. Stroescu, A. Stoica-Guzun, S. Ghergu, N. Chira, I. Jipa, Optimization of fatty acids extraction from Portulaca oleracea seed using response surface methodology, Ind. Crops Prod., 43 (2013) 405–411.
[24] G.J. Swamy, A. Sangamithra, V. Chandrasekar, Response surface modeling and process optimization of aqueous extraction of natural pigments from Beta vulgaris using Box–Behnken design of experiments, Dyes Pigm., 111 (2014) 64–74.
[25] M. Ginni, S.A. Kumar, J.R. Banu, I.T. Yeom, Synergistic photodegradation of pulp and paper mill wastewater by combined advanced oxidation process, Desal. Wat. Treat., 68 (2017) 160–169.
[26] V.G. Sharmila, P. Dhanalakshmi, J.R. Banu, S. Kavitha, M. Gunasekaran, Effect of deflocculation on photo induced thin layer titanium dioxide disintegration of dairy waste activated sludge for cost and energy efficient methane production, Bioresour. Technol., 244 (2017) 776–784.
[27] V. Amudhaa, J.R. Banua, I.T. Yeomb, Efficiency of zero valent iron in the modified Fenton process for the reduction of excess sludge and the key role of citric acid through deflocculation, Desal. Wat. Treat., 71 (2017) 271–279.
[28] S. Asokapandian, S. Venkatachalam, G.J. Swamy, K. Kuppusamy, Optimization of foaming properties and foam mat drying of muskmelon using soy protein, J. Food Process Eng., 39 (2016) 692–701.
[29] G. Sokkanathan, V.G. Sharmila, S. Kaliappan, J.R. Banu, I.T. Yeom, R.U. Rani, Combinative treatment of phenol-rich retting-pond wastewater by a hybrid upflow anaerobic sludge blanket reactor and solar photofenton process, J. Environ. Manage., 206 (2018) 999–1006.
[30] J. Joshi, M.M. Sharma, Mass transfer and hydrodynamic characteristics of gas inducing type of agitated contactors, Can. J. Chem. Eng., 55 (1977) 683–695.
[31] J. Kim, G.Y. Han, Effect of agitation on fluidization characteristics of fine particles in a fluidized bed, Powder Technol., 166 (2006) 113–122.